Extended Abstracts of the 2007 International Conference on Solid State Devices and Materials, Tsukuba, 2007, pp. 498-499

P-5-10

UWB Transmission Characteristics of Bow-tie Antennas on Si

S. Kubota*, Xia Xiao, K. Kimoto and T. Kikkawa

Research Center for Nanodevices and Systems, Hiroshima University
1-4-2 Kagamiyama, Higashi-hiroshima, Hiroshima 739-8527, Japan.
Phone: +81-82-424-7879, Fax: +81-82-424-3499, E-mail: kikkawa@sxsys.hiroshima-u.ac.jp

1. Introduction

UWB(ultrawide-band) is a carrierless short range communication technology which transmits the information in the form of very short pulses.[1] UWB can offer high data rates at short distances with low power, primarily due to wide bandwidth. Compact and cheap UWB antennas [2-4] are needed for numerous UWB applications like wireless communication, stacked-LSI packaging, indoor positioning and medical imaging.

In this paper, we fabricate bow-tie antennas on Si substrates as shown in Fig.1 to investigate on-chip integrated antenna characteristics for single chip UWB transceiver. We investigate the UWB transmission characteristics of bow-tie antennas by evaluating the influence of the antenna length, flare angle and the resistivity of the Si substrates on the reflection and transmission coefficients.

2. Experimental

P-type (100) Si wafers with resistivities (ρ) of 10 Ω·cm, 79.6 Ω·cm and 2.29 kΩ·cm were prepared as substrates, whose thicknesses were 260 μm. The surface of Si wafer was oxidized to form 0.3 μm-thick field SiO_2. 1.0 μm-thick aluminum was deposited on the SiO_2 layer by direct current magnetron sputtering and the antenna patterns were formed by electron beam lithography followed by wet etching. A bow-tie antenna fabricated on the SiO_2 layer. The bow-tie antennas with flare angle (θ) of 53° whose antenna length (L) changed from 3.58 mm to 7.16 mm were fabricated. The bow-tie antennas with constant diagonal length were also fabricated, whose lengths (L) changed from 6 mm to 4.24 mm and flare angles changed from 0° to 90°. The distance between transmitting and receiving antennas was 10 mm.

The measurement sample was placed on a 2.6 mm-thick low-k substrate whose dielectric constant was 2.15 at 1 GHz [3]. Fig. 2 and Fig. 3 show sample structures for intra-chip and inter-chip transmission characteristics, respectively. For inter-chip measurement, the distance between transmitting and receiving antennas was 20 mm.

Scattering parameter measurement set-up in frequency domain is composed of a vector network analyzer HP8510C, 180° hybrid couplers (6-26.5 GHz), signal-signal (SS) probes and a microwave probe station. Fig. 4 shows measurement set-up for transmission of Gaussian monocycle pulse (GMP). It consists of Agilent 4902B serial bit error rate tester (BERT), Picosecond impulse forming networks, Agilent 86100C sampling oscilloscope and a microwave probe station. Rectangular pulses were transformed to Gaussian monocycle pulse trains by use of two impulse forming networks. Resulting peak-to-peak voltage was 140 mV.

3. Result and discussion

Fig. 5 shows reflection (S_{11}) and transmission (S_{21}) coefficients versus antenna length, with flare angle of 53° for intra-chip transmission at 15 GHz. S_{11} decreased as antenna length increased. S_{21} increased with antenna length, and S_{21} was -22 dB for L = 7.16 mm and ρ = 79.6 Ω·cm. Fig. 6 shows S_{11} and S_{21} versus flare angle for intra-chip transmission at 15 GHz. S_{11} was less than -10 dB for $\theta \geq 53°$. S_{21} was constant for $\theta \geq 37°$ because the diagonal length were the same, and S_{21} was -22 dB for ρ = 79.6 Ω·cm. Fig. 7 shows S_{11} and S_{21} versus the resistivity of Si substrate for intra-chip transmission at 15 GHz. S_{11} and S_{21} increased as the resistivity increased. Figs. 8-10 show S_{11} and S_{21} versus antenna length, Flare angle, and the resistivity of Si substrate for inter-chip transmission, respectively. Similar characteristics to intra-chip transmission were observed, and S_{21} was -27 dB for L = 7.16 mm, θ = 53° and ρ = 79.6 Ω·cm. Fig. 11 shows intra-chip received waveforms, for the resistivities of 10 Ω·cm, 79.6 Ω·cm and 2.29 kΩ·cm. The amplitude increased with increasing the resistivity of Si substrate while the waveforms were the similar. Fig. 12 shows intra-chip frequency spectra of received waveforms calculated by FFT (Fast Fourier Transformation). The dominant frequency component was 20 GHz. Fig. 13 shows inter-chip received waveforms. Similar to intra-chip, the amplitude increased with increasing the resistivity of Si substrate. Fig. 14 shows intra-chip frequency spectra of the received waveforms. The dominant frequency component was 13 GHz due to the difference in the dielectric constants of air in comparison with Si substrate. Fig. 15 shows peak-to-peak voltage versus the resistivity of Si substrate. Peak-to-peak voltages for intra-chip and inter-chip improved from 1.8 and 1.3 mV to 11.5 and 4.8 mV, respectively, by increasing the substrate resistivity from 10 Ω·cm to 2.29 kΩ·cm.

3. Conclusions

The gain of bow-tie antenna increased with increasing antenna length and the resistivity of Si substrate. The gain did not depend on the flare angle when the diagonal length was the same. The frequency spectra of GMP were different between intra- and inter- chip transmissions due to the difference in transmission media.

References

[1]P. K. Saha et al., 2006 Symposium on VLSI circuits Dig. Tech. Papers, pp.252-253, (Honolulu, June 15-17) 2006.
[2]A.B.M. H. Rashid et al., Applied physics. Lett. **23** (2002) 731.
[3]T. Kikkawa et al., IEEE Electron Device Lett. **26** (2005) 767.
[4] K. Kimoto et al., Jap. J. Appl. Phys. **45** (2006) 4968.

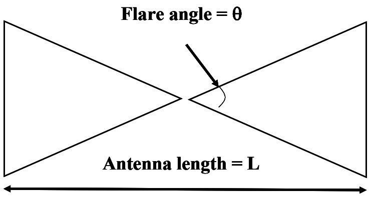

Fig. 1. Structure of bow-tie antenna.

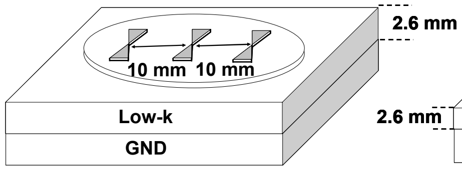

Fig. 2. Intra-chip sample structure.

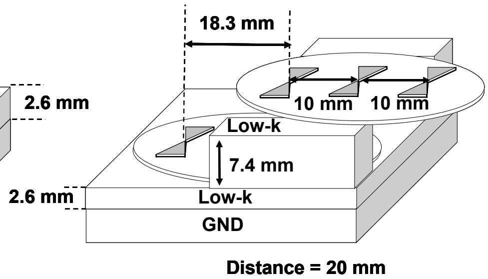

Fig. 3. Inter-chip sample structure.

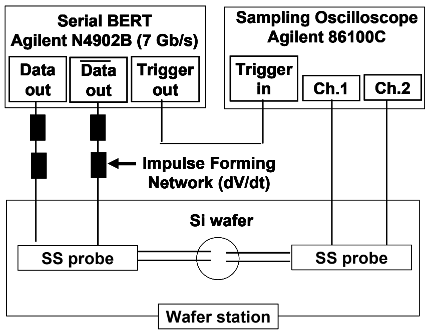

Fig. 4. Measurement set-up for transmission characteristics of GMP.

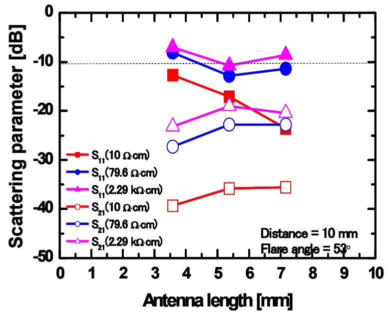

Fig. 5. Intra-chip scattering parameter at 15 GHz versus antenna length.

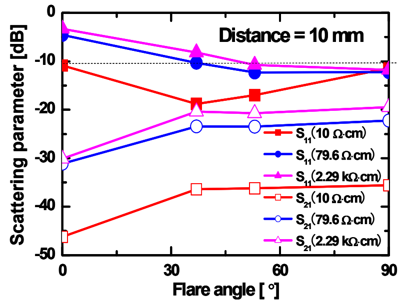

Fig. 6. Intra-chip scattering parameter at 15 GHz versus flare angle.

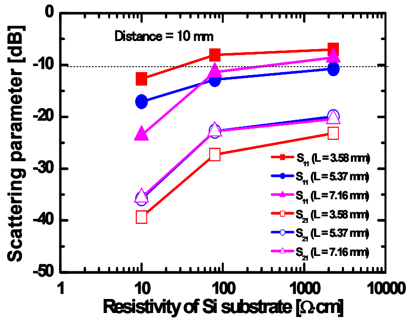

Fig. 7. Intra-chip scattering parameter at 15 GHz versus the resistivity of Si.substrate.

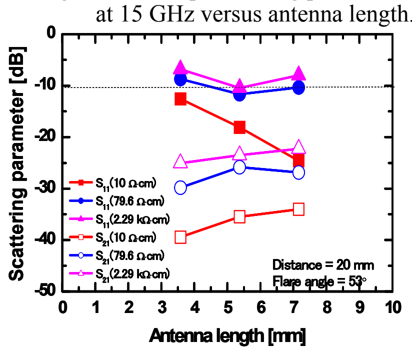

Fig. 8. Inter-chip scattering parameter at 15 GHz versus antenna length.

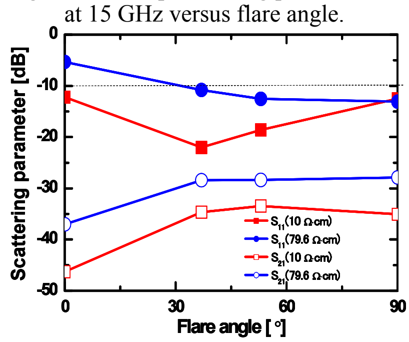

Fig. 9. Inter-chip scattering parameter at 15 GHz versus flare angle.

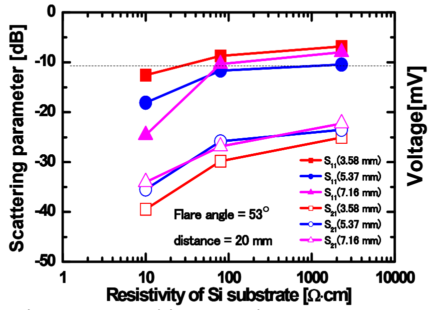

Fig. 10. Inter-chip scattering parameter at 15 GHz versus the resistivity of Si.substrate.

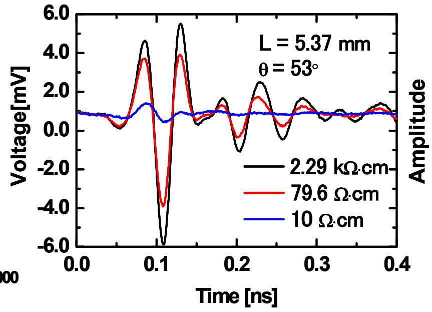

Fig. 11. Intra-chip received waveforms.

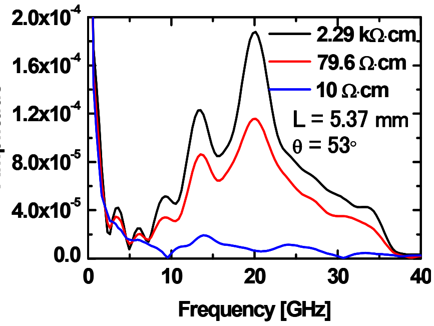

Fig. 12. Intra-chip frequency spectra of received waveforms.

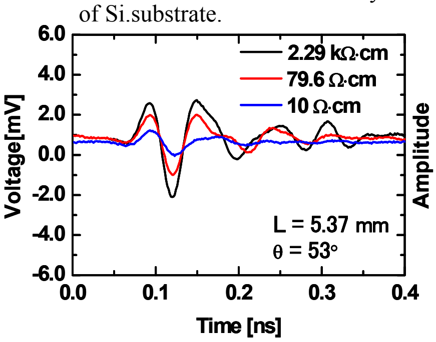

Fig. 13. Inter-chip received waveforms.

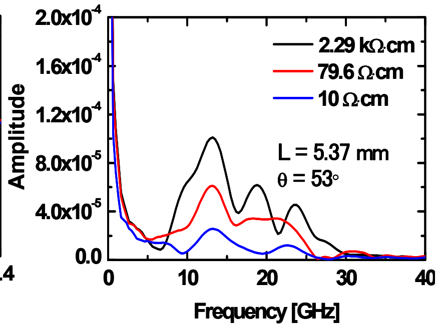

Fig. 14. Inter-chip frequency spectra of received waveforms.

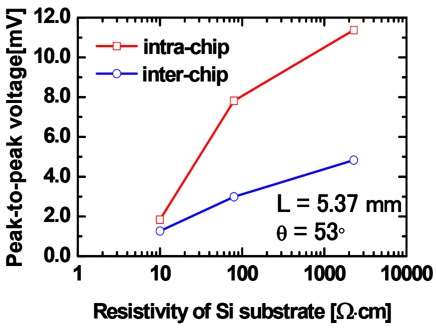

Fig. 15. Peak-to-peak voltage versus resistivity of Si substrate.